Lattice study of the confinement/deconfinement transition in rotating gluodynamics

V. V. Braguta[1,2,3], A. Yu. Kotov[4], D. D. Kuznedelev[3], A. A. Roenko[1]

[1]Joint Institute for Nuclear Research, Bogoliubov Laboratory of Theoretical Physics
[2]National University of Science and Technology MISiS
[3]Moscow Institute of Physics and Technology
[4]Jülich Supercomputing Centre

LATTICE21, ZOOM/GATHER@MIT, 28 July 2021

- In non-central heavy ion collisions creation of QGP with angular momentum is expected.

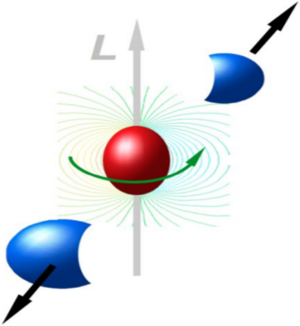

- In non-central heavy ion collisions creation of QGP with angular momentum is expected.
- The rotation occurs with relativistic velocities.

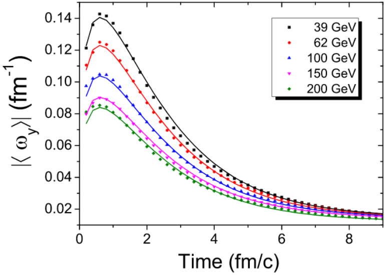

Au+Au, $b = 7$ fm

[Y. Jiang, Z.-W. Lin, and J. Liao, Phys. Rev. C **94**, 044910 (2016), arXiv:1602.06580 [hep-ph]]

$\omega \sim 0.1 - 0.2\,\mathrm{fm}^{-1} \sim 20 - 40$ MeV

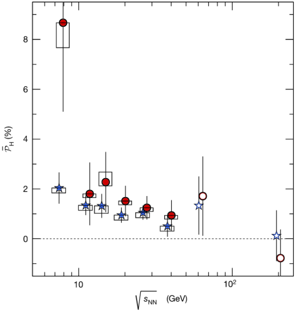

[L. Adamczyk et al. (STAR), Nature **548**, 62–65 (2017), arXiv:1701.06657 [nucl-ex]]

$\omega \sim 6$ MeV

Introduction

- In non-central heavy ion collisions creation of QGP with angular momentum is expected.
- The rotation occurs with relativistic velocities.

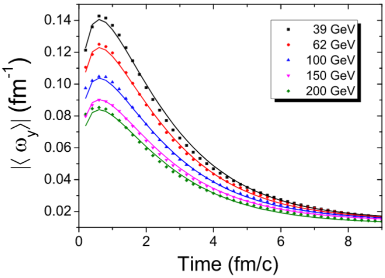

Au+Au, $b = 7$ fm

[Y. Jiang, Z.-W. Lin, and J. Liao, Phys. Rev. C **94**, 044910 (2016), arXiv:1602.06580 [hep-ph]]

$\omega \sim 0.1 - 0.2\,\text{fm}^{-1} \sim 20 - 40$ MeV

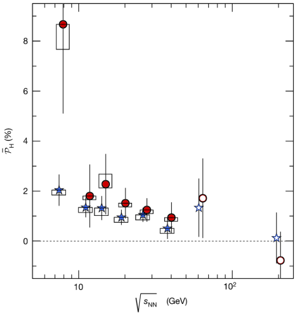

[L. Adamczyk et al. (STAR), Nature **548**, 62–65 (2017), arXiv:1701.06657 [nucl-ex]]

$\omega \sim 6$ MeV

- How does the rotation affect to phase transitions in QCD?

Related papers

Rotation on the lattice (phase transitions were not considered):

- A. Yamamoto and Y. Hirono, Phys. Rev. Lett. **111**, 081601 (2013), arXiv:1303.6292 [hep-lat]

Related papers

Rotation on the lattice (phase transitions were not considered):

- A. Yamamoto and Y. Hirono, Phys. Rev. Lett. **111**, 081601 (2013), arXiv:1303.6292 [hep-lat]

Properties of rotating QCD matter (mostly within NJL, focused on fermions):

- S. Ebihara, K. Fukushima, and K. Mameda, Phys. Lett. B **764**, 94–99 (2017), arXiv:1608.00336 [hep-ph]
- M. Chernodub and S. Gongyo, JHEP **01**, 136 (2017), arXiv:1611.02598 [hep-th]
- X. Wang, M. Wei, Z. Li, and M. Huang, Phys. Rev. D **99**, 016018 (2019), arXiv:1808.01931 [hep-ph]
- H. Zhang, D. Hou, and J. Liao, Chin. Phys. C **44**, 111001 (2020), arXiv:1812.11787 [hep-ph]
- ...
- Y. Jiang and J. Liao, Phys. Rev. Lett. **117**, 192302 (2016), arXiv:1606.03808 [hep-ph]

Rotation suppress the chiral condensate (state with $S = 0$)

- Holography: X. Chen et al., (2020), arXiv:2010.14478 [hep-ph]
- Compact QED in 2+1-D M. N. Chernodub, Phys. Rev. D **103**, 054027 (2021), arXiv:2012.04924 [hep-ph]
- HRG model: Y. Fujimoto, K. Fukushima, and Y. Hidaka, Phys. Lett. B **816**, 136184 (2021), arXiv:2101.09173 [hep-ph]

Related papers

Rotation on the lattice (phase transitions were not considered):

- A. Yamamoto and Y. Hirono, Phys. Rev. Lett. **111**, 081601 (2013), arXiv:1303.6292 [hep-lat]

Properties of rotating QCD matter (mostly within NJL, focused on fermions):

- S. Ebihara, K. Fukushima, and K. Mameda, Phys. Lett. B **764**, 94–99 (2017), arXiv:1608.00336 [hep-ph]
- M. Chernodub and S. Gongyo, JHEP **01**, 136 (2017), arXiv:1611.02598 [hep-th]
- X. Wang, M. Wei, Z. Li, and M. Huang, Phys. Rev. D **99**, 016018 (2019), arXiv:1808.01931 [hep-ph]
- H. Zhang, D. Hou, and J. Liao, Chin. Phys. C **44**, 111001 (2020), arXiv:1812.11787 [hep-ph]
- ...
- Y. Jiang and J. Liao, Phys. Rev. Lett. **117**, 192302 (2016), arXiv:1606.03808 [hep-ph]

Rotation suppress the chiral condensate (state with $S = 0$)

- Holography: X. Chen et al., (2020), arXiv:2010.14478 [hep-ph]
- Compact QED in 2+1-D M. N. Chernodub, Phys. Rev. D **103**, 054027 (2021), arXiv:2012.04924 [hep-ph]
- HRG model: Y. Fujimoto, K. Fukushima, and Y. Hidaka, Phys. Lett. B **816**, 136184 (2021), arXiv:2101.09173 [hep-ph]

$\Rightarrow$ Critical temperature decreases due to the rotation.

Rotating reference frame

- SU(3)-gluodynamics (at thermal equilibrium) is investigated in the reference frame which rotates with the system with angular velocity Ω .
- In this reference frame there appears an external gravitational field

$$g_{\mu\nu} = \begin{pmatrix} 1 - r^2\Omega^2 & \Omega y & -\Omega x & 0 \\ \Omega y & -1 & 0 & 0 \\ -\Omega x & 0 & -1 & 0 \\ 0 & 0 & 0 & -1 \end{pmatrix} .$$

- The partition function is[1]

$$Z = \mathrm{Tr} \exp \left[-\beta \hat{H} \right] \qquad \Rightarrow \qquad Z = \int DA \, \exp\left(-S_G\right) , \tag{1}$$

where the Euclidean action can be written as

$$S_G = \frac{1}{2g^2} \int d^4x \, \sqrt{g_E} \, g_E^{\mu\nu} g_E^{\alpha\beta} F^a_{\mu\alpha} F^a_{\nu\beta} .$$

[1] A. Yamamoto and Y. Hirono, Phys. Rev. Lett. **111**, 081601 (2013), arXiv:1303.6292 [hep-lat].

- Tolman-Ehrenfest effect: In gravitational field the temperature isn't a constant in space at thermal equilibrium:

$$T(r)\sqrt{g_{00}} = const\,,$$

Rotating reference frame: temperature

- Tolman-Ehrenfest effect: In gravitational field the temperature isn't a constant in space at thermal equilibrium:

$$T(r)\sqrt{g_{00}} = const\,,$$

- For the rotation one has

$$T(r)\sqrt{1 - r^2\Omega^2} = const \equiv T\,,$$

- One could expect, that the rotation effectively warm up the periphery of the modeling volume

$$T(r) > T(r = 0),$$

and as a result, from kinematics, the critical temperature should decreases.

Rotating reference frame

The Euclidean action can be written as

$$S_G = \frac{1}{4g^2}\int d^4x\,\sqrt{g_E}\,g_E^{\mu\nu}\,g_E^{\alpha\beta}\,F^a_{\mu\alpha}F^a_{\nu\beta}\,. \tag{2}$$

Substituting the $(g_E)_{\mu\nu}$ to formula (2) one gets

$$S_G = \frac{1}{2g^2}\int d^4x\,\Big[(1-r^2\Omega^2)F^a_{xy}F^a_{xy} + (1-y^2\Omega^2)F^a_{xz}F^a_{xz} + (1-x^2\Omega^2)F^a_{yz}F^a_{yz} + \\ + F^a_{x\tau}F^a_{x\tau} + F^a_{y\tau}F^a_{y\tau} + F^a_{z\tau}F^a_{z\tau} - \\ - 2iy\Omega(F^a_{xy}F^a_{y\tau} + F^a_{xz}F^a_{z\tau}) + 2ix\Omega(F^a_{yx}F^a_{x\tau} + F^a_{yz}F^a_{z\tau}) - 2xy\Omega^2 F^a_{xz}F^a_{zy}\Big]\,.$$

Rotating reference frame

The Euclidean action can be written as

$$S_G = \frac{1}{4g^2} \int d^4x \, \sqrt{g_E} \, g_E^{\mu\nu} \, g_E^{\alpha\beta} \, F^a_{\mu\alpha} F^a_{\nu\beta} \, . \qquad (2)$$

Substituting the $(g_E)_{\mu\nu}$ to formula (2) one gets

$$S_G = \frac{1}{2g^2} \int d^4x \, \Big[(1 - r^2\Omega^2) F^a_{xy} F^a_{xy} + (1 - y^2\Omega^2) F^a_{xz} F^a_{xz} + (1 - x^2\Omega^2) F^a_{yz} F^a_{yz} + \\ + F^a_{x\tau} F^a_{x\tau} + F^a_{y\tau} F^a_{y\tau} + F^a_{z\tau} F^a_{z\tau} - \\ - 2iy\Omega (F^a_{xy} F^a_{y\tau} + F^a_{xz} F^a_{z\tau}) + 2ix\Omega (F^a_{yx} F^a_{x\tau} + F^a_{yz} F^a_{z\tau}) - 2xy\Omega^2 F^a_{xz} F^a_{zy} \Big] \, .$$

Sign problem

- The Euclidean action is complex-valued function!
- The Monte–Carlo simulations are conducted with imaginary angular velocity $\Omega_I = -i\Omega$.
- The results are analytically continued to the region of the real angular velocity.

Lattice action

The lattice action can be written as

$$S_G = \beta \sum_x \Big((1 + r^2\Omega_I^2)(1 - \frac{1}{N_c}\text{Re Tr } \bar{U}_{xy}) + (1 + y^2\Omega_I^2)(1 - \frac{1}{N_c}\text{Re Tr } \bar{U}_{xz}) +$$

$$+ (1 + x^2\Omega_I^2)(1 - \frac{1}{N_c}\text{Re Tr } \bar{U}_{yz}) + 3 - \frac{1}{N_c}\text{Re Tr } (\bar{U}_{x\tau} + \bar{U}_{y\tau} + \bar{U}_{z\tau}) -$$

$$- \frac{1}{N_c}\text{Re Tr } \big(y\Omega_I(\bar{V}_{xy\tau} + \bar{V}_{xz\tau}) - x\Omega_I(\bar{V}_{yx\tau} + \bar{V}_{yz\tau}) + xy\Omega_I^2 \bar{V}_{xzy} \big) \Big),$$

where $\beta = 2N_c/g^2$,

$\bar{U}_{\mu\nu}$ denotes clover-type average of four plaquettes,

$\bar{V}_{\mu\nu\rho}$ is asymmetric chair-type average of 8 chair.

$\bar{U}_{\mu\nu} = \frac{1}{4}$

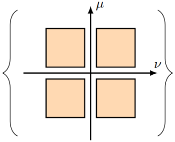

$\bar{V}_{\mu\nu\rho} = \frac{1}{8}$

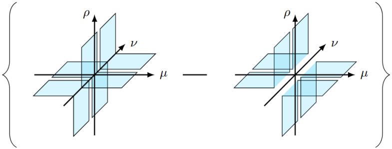

Lattice setup

- Simulation is performed on the lattice $N_t \times N_z \times N_s^2$ $(N_s = N_x = N_y)$, which rotates around z-axis.
- The system should be limited in the directions, which are orthogonal to the rotation axis: $\Omega_I (N_s - 1) a / \sqrt{2} < 1$

Lattice setup

- Simulation is performed on the lattice $N_t \times N_z \times N_s^2 \ \ (N_s = N_x = N_y)$, which rotates around z-axis.
- The system should be limited in the directions, which are orthogonal to the rotation axis: $\Omega_I (N_s - 1) a/\sqrt{2} < 1$

$$\Downarrow$$

- The boundary conditions in directions x, y have to be treated carefully! The results depend on BC for any approach. (PBC are used in directions t, z.)

Lattice setup

- Simulation is performed on the lattice $N_t \times N_z \times N_s^2$ $(N_s = N_x = N_y)$, which rotates around z-axis.
- The system should be limited in the directions, which are orthogonal to the rotation axis: $\Omega_I (N_s - 1) a/\sqrt{2} < 1$

$$\Downarrow$$

- The boundary conditions in directions x, y have to be treated carefully! The results depend on BC for any approach. (PBC are used in directions t, z.)

The following types of BC were systematically checked:

- Open b.c. – OBC
  - All $U_{\mu\nu}$, $V_{\mu\nu\rho}$, which contain links sticking out of the lattice, excluded.
  - Does not break any symmetries.
  - $U_P = 1$ for all $P \in$ out; or $F_{\mu\nu} = 0$ $\Rightarrow$ „low“ temperature on the boundary.

Lattice setup

- Simulation is performed on the lattice $N_t \times N_z \times N_s^2$ $(N_s = N_x = N_y)$, which rotates around z-axis.
- The system should be limited in the directions, which are orthogonal to the rotation axis: $\Omega_I (N_s - 1) a/\sqrt{2} < 1$

$$\Downarrow$$

- The boundary conditions in directions x, y have to be treated carefully! The results depend on BC for any approach. (PBC are used in directions t, z.)

The following types of BC were systematically checked:

- Open b.c. – OBC
  - All $U_{\mu\nu}$, $V_{\mu\nu\rho}$, which contain links sticking out of the lattice, excluded.
  - Does not break any symmetries.
  - $U_P = 1$ for all $P \in$ out; or $F_{\mu\nu} = 0$ $\Rightarrow$ „low“ temperature on the boundary.
- Periodic b.c. – PBC
  - The velocity distribution is not periodic.

Lattice setup

- Simulation is performed on the lattice $N_t \times N_z \times N_s^2$ $(N_s = N_x = N_y)$, which rotates around z-axis.
- The system should be limited in the directions, which are orthogonal to the rotation axis: $\Omega_I (N_s - 1)a/\sqrt{2} < 1$

$$\Downarrow$$

- The boundary conditions in directions x, y have to be treated carefully! The results depend on BC for any approach. (PBC are used in directions t, z.)

The following types of BC were systematically checked:

- Open b.c. – OBC
  - All $U_{\mu\nu}$, $V_{\mu\nu\rho}$, which contain links sticking out of the lattice, excluded.
  - Does not break any symmetries.
  - $U_P = 1$ for all $P \in$ out; or $F_{\mu\nu} = 0$ $\Rightarrow$ „low“ temperature on the boundary.
- Periodic b.c. – PBC
  - The velocity distribution is not periodic.
- Dirichlet b.c. – DBC
  - $U_\mu(x) = \hat{1}$ for all $x, x + \mu \in$ boundary
  - Violate $\mathbb{Z}_3$ center symmetry.
  - $L(x, y) = 3$ on the boundary $\Rightarrow$ „high“ temperature on the boundary.

Polyakov loop

The Polyakov loop is an order parameter. The lattice version is defined as usual:

$$L(\vec{x}) = \mathrm{Tr}\left[\prod_{\tau=0}^{N_t-1} U_4(\vec{x},\tau)\right], \qquad L = \frac{1}{N_s^2 N_z}\sum_{\vec{x}} L(\vec{x})\,. \tag{3}$$

In confinement $\langle L\rangle = 0$; in deconfinement $\langle L\rangle \neq 0$ ($\mathbb{Z}_3$ center symmetry is broken).

The critical temperature T_c is determined using the Polyakov loop susceptibility

$$\chi = N_s^2 N_z \left(\langle |L|^2\rangle - \langle |L|\rangle^2\right), \tag{4}$$

by means of the Gaussian fit.

- Non-periodic b.c. changes the critical temperature $T_c(0)$
  - $T_c(0)^{OBC} > T_c(0)^{PBC}$
  - $T_c(0)^{DBC} < T_c(0)^{PBC}$
- With $N_s/N_t \to \infty$ their influence wanes, and $T_c(0) \to T_c(0)^{(PBC)}$

Open boundary conditions

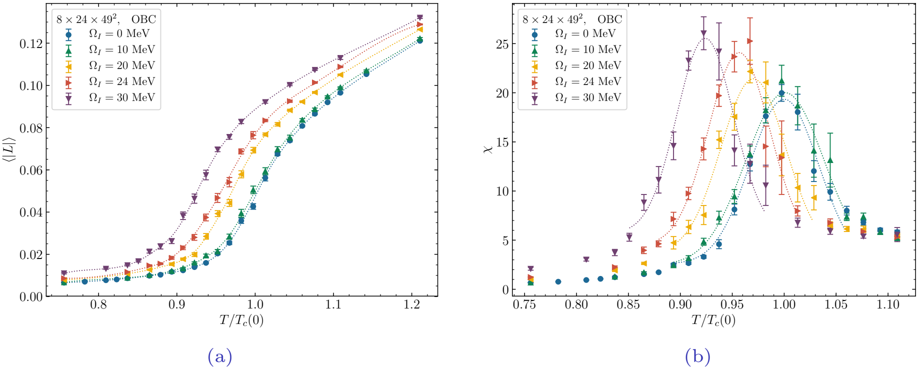

Figure: The Polyakov loop (a) and Polyakov loop susceptibility (b) as a function of temperature for different values of imaginary angular velocity Ω_I. The results are obtained on the lattice $8 \times 24 \times 49^2$.

Open boundary conditions: critical temperature

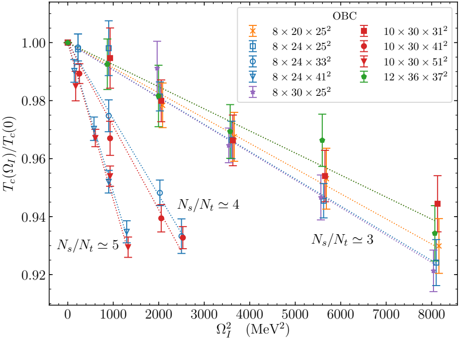

T_c depends on Ω_I^2 and is well described by

$$\frac{T_c(\Omega_I)}{T_c(0)} = 1 - C_2\Omega_I^2$$

- The coefficient C_2 depends on the transverse lattice size (N_s/N_t) and almost independent of both the lattice spacing and the lattice size along the rotation axis (N_z/N_t).

Open boundary conditions: critical temperature

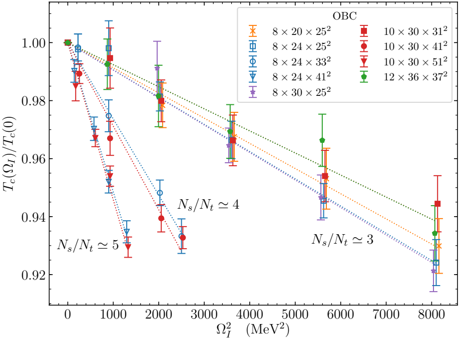

T_c depends on Ω_I^2 and is well described by

$$\frac{T_c(\Omega_I)}{T_c(0)} = 1 - C_2 \Omega_I^2$$

$$\Downarrow \quad (\Omega_I^2 = -\Omega^2)$$

$$\frac{T_c(\Omega)}{T_c(0)} = 1 + C_2 \Omega^2$$

The critical temperature increases with the angular velocity ($C_2 > 0$)

- The coefficient C_2 depends on the transverse lattice size (N_s/N_t) and almost independent of both the lattice spacing and the lattice size along the rotation axis (N_z/N_t).

Open boundary conditions: critical temperature

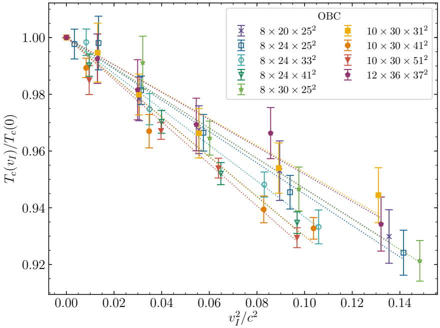

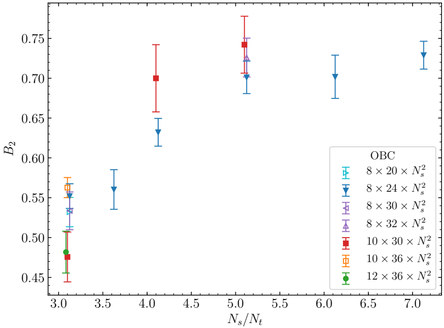

The linear velocity on the boundary $v_I = \Omega_I \,(N_s - 1)\, a(\beta_c)/2$

$$\frac{T_c(v_I)}{T_c(0)} = 1 - B_2 \frac{v_I^2}{c^2} \qquad \Longrightarrow \qquad \frac{T_c(v)}{T_c(0)} = 1 + B_2 \frac{v^2}{c^2}$$

- The coefficient B_2 slightly depends on the transverse lattice size (N_s/N_t).
- For lattices with sufficiently large N_s and OBC the coefficient is $B_2 \sim 0.7$.

Periodic boundary conditions: critical temperature

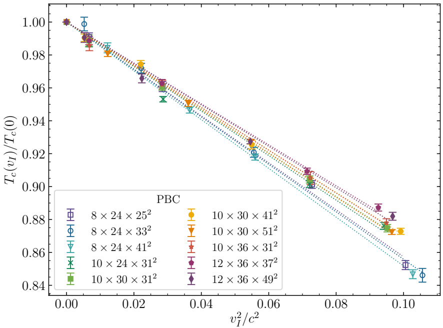

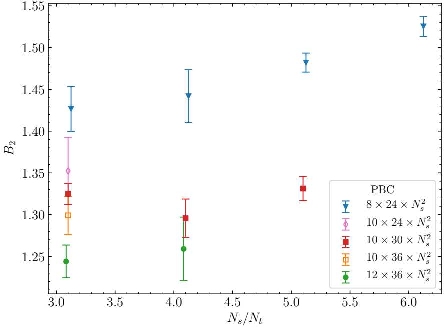

The linear velocity on the boundary $v_I = \Omega_I\,(N_s - 1)\,a(\beta_c)/2$

$$\frac{T_c(v_I)}{T_c(0)} = 1 - B_2 \frac{v_I^2}{c^2} \qquad \Longrightarrow \qquad \frac{T_c(v)}{T_c(0)} = 1 + B_2 \frac{v^2}{c^2}$$

- The results for the finest lattices with $N_t = 10, 12$ are close to each others, and for PBC the coefficient is $B_2 \sim 1.3$.

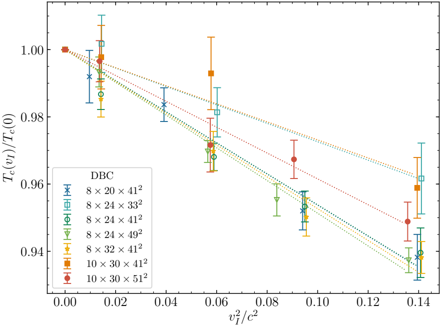

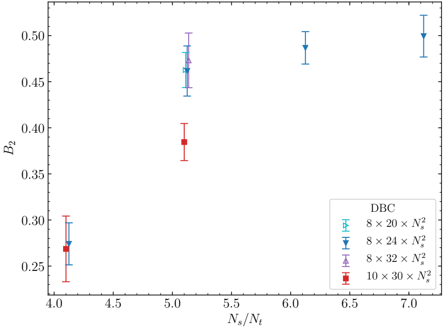

The linear velocity on the boundary $v_I = \Omega_I \, (N_s - 1) \, a(\beta_c)/2$

$$\frac{T_c(v_I)}{T_c(0)} = 1 - B_2 \frac{v_I^2}{c^2} \qquad \Longrightarrow \qquad \frac{T_c(v)}{T_c(0)} = 1 + B_2 \frac{v^2}{c^2}$$

- For lattices with sufficiently large N_s and DBC the coefficient goes to plateau $B_2 \sim 0.5$.

Rotation and susceptibility scaling

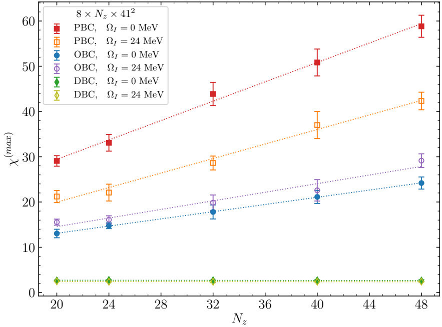

Figure: The height of the susceptibility peak for various lattices $8 \times N_z \times 41^2$ and zero/nonzero angular velocities.

Rotation does not change the order of the phase transition (in studied region of Ω):

- OBC: $\chi^{(max)} \sim V$
- PBC: $\chi^{(max)} \sim V$
- DBC: $\chi^{(max)} \sim const$

The rotation affect both gluon and fermionic degrees of freedom.

$$Z = \int D\psi \, D\bar{\psi} \, DA \, \exp\big(-S_G[A,\Omega] - S_F[\bar{\psi},\psi,A,\Omega]\big)\,. \quad (5)$$

Including fermions (preliminary results)

The rotation affect both gluon and fermionic degrees of freedom.

$$Z = \int D\psi\, D\bar{\psi}\, DA \exp\left(- S_G[A,\Omega] - S_F[\bar{\psi},\psi,A,\Omega]\right). \qquad (5)$$

There is the sign problem for the lattice quark action. After the same substitution ($\Omega = -i\Omega_I$) it has the following form

$$S_F = \sum_{x_1,x_2} \bar{\psi}(x_1) \Bigg\{ \delta_{x_1,x_2} - \kappa \Big[(1-\gamma^x) T_{x+} + (1+\gamma^x) T_{x-} + (1-\gamma^y) T_{y+} + (1+\gamma^y) T_{y-} + (1-\gamma^z) T_{z+} + (1+\gamma^z) T_{z-} + (1-\gamma^\tau) \exp\left(ia\Omega_I \frac{\sigma^{12}}{2}\right) T_{\tau+} + (1+\gamma^\tau) \exp\left(-ia\Omega_I \frac{\sigma^{12}}{2}\right) T_{\tau-} \Big] \Bigg\} \psi(x_2), \qquad (6)$$

where $T_{\mu+} = U_\mu(x_1)\delta_{x_1+\mu,x_2}$, $T_{\mu-} = U_\mu(x_1)\delta_{x_1-\mu,x_2}$ and

$$\gamma^x = \gamma^1 - y\Omega_I\gamma^4, \quad \gamma^y = \gamma^2 + x\Omega_I\gamma^4, \quad \gamma^z = \gamma^3, \quad \gamma^\tau = \gamma^4.$$

The Monte-Carlo simulations with dynamical fermions ($N_f = 2$ Wilson fermions) for an imaginary angular velocity were performed.

Rotating QCD

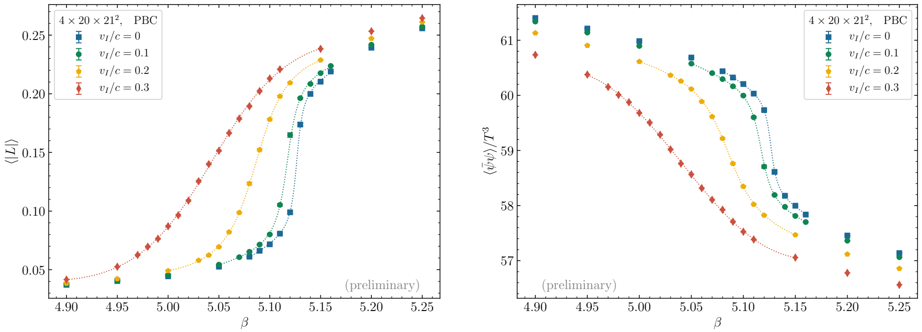

(a) (b)

Figure: The Polyakov loop (a) and the chiral condensate (b) as a function of β for different values of imaginary angular velocity Ω_I. Lattice $4 \times 20 \times 21^2$, the hopping parameter $\kappa = 0.170$ ($m_\pi \simeq 690$ MeV, $T \simeq 171$ MeV for $\beta = 5.15$).

- Critical couplings β_c for chiral transition and confinement-deconfinement transition coincide with each other (up to the error).

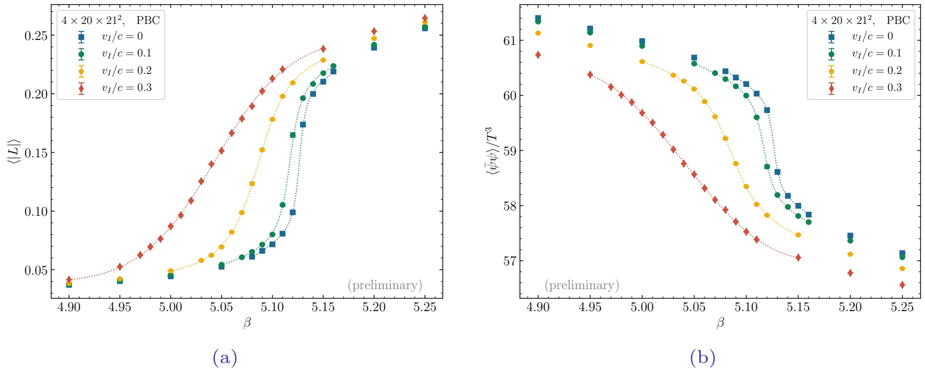

Figure: The Polyakov loop (a) and the chiral condensate (b) as a function of β for different values of imaginary angular velocity Ω_I. Lattice $4 \times 20 \times 21^2$, the hopping parameter $\kappa = 0.170$ ($m_\pi \simeq 690$ MeV, $T \simeq 171$ MeV for $\beta = 5.15$).

- Critical couplings β_c for chiral transition and confinement-deconfinement transition coincide with each other (up to the error).

One can split the full action as $S_G(\Omega_G) + S_F(\Omega_F)$ and rotate each part separately!

Rotating QCD

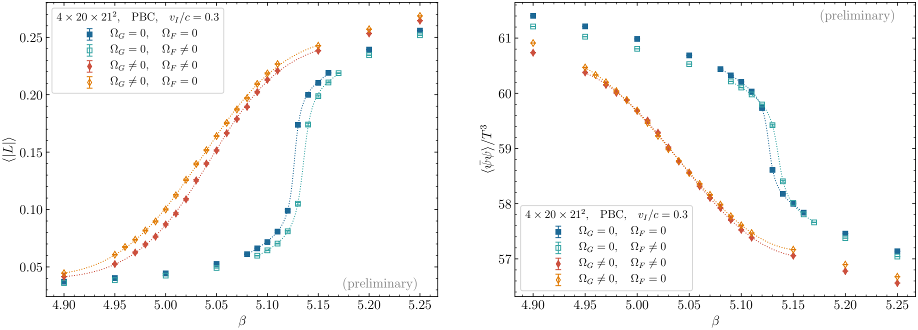

(a) (b)

Figure: The Polyakov loop (a) and the chiral condensate (b) as a function of β for different values of imaginary angular velocity Ω_I. Lattice $4 \times 20 \times 21^2$, the hopping parameter $\kappa = 0.170$.

- Rotation of fermions and gluons separately has the opposite influence on the critical coupling (temperature).

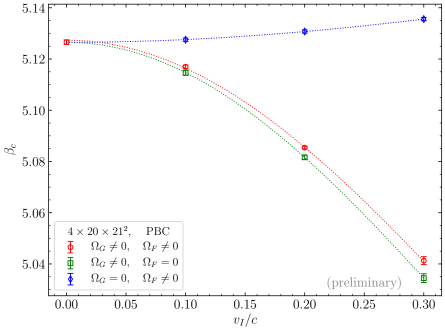

Figure: The critical value β_c as function of imaginary linear velocity on the boundary.

- Rotation of fermions and gluons separately has the opposite influence on the critical coupling (temperature).

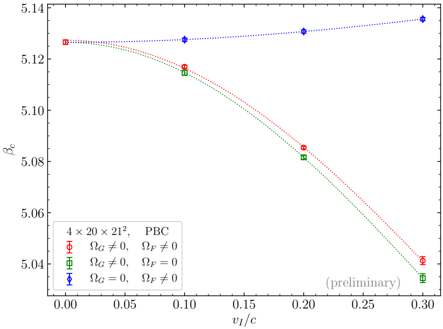

Figure: The critical value β_c as function of imaginary linear velocity on the boundary.

- Rotation of fermions and gluons separately has the opposite influence on the critical coupling (temperature).
- The results are qualitatively the same for OBC.

Conclusions

- The critical temperature of the confinement/deconfinement transition in gluodynamics increases with angular velocity

$$\frac{T_c(\Omega)}{T_c(0)} = 1 + C_2\Omega^2 ,$$

- The result does not depend on the boundary condition used

$$\frac{T_c(v)}{T_c(0)} = 1 + B_2\frac{v^2}{c^2} ,$$

  where for OBC $B_2 \sim 0.7$, for PBC $B_2 \sim 1.3$ and for DBC $B_2 \sim 0.5$
- Rotation does not change the order of the phase transition.
- It should be noted, that NJL (and other phenomenological models) predicts that critical temperature decreases due to the rotation.
- Preliminary results for QCD show that the separate rotation of quarks and gluons has the opposite influence on β_c (for $m_\pi \sim 690$ MeV gluons win).

See the details in:

- V. V. Braguta, A. Y. Kotov, D. D. Kuznedelev, and A. A. Roenko, Phys. Rev. D **103**, 094515 (2021), arXiv:2102.05084 [hep-lat]
- V. V. Braguta, A. Y. Kotov, D. D. Kuznedelev, and A. A. Roenko, JETP Lett. **112**, 6–12 (2020)

Thank you for your attention!

Open boundary conditions

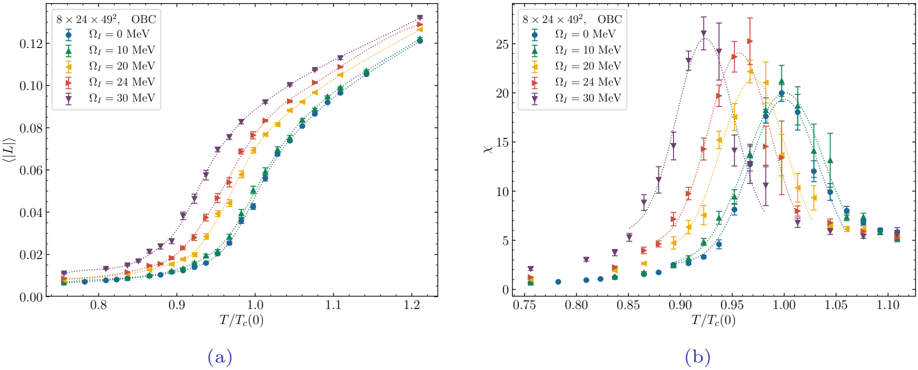

Figure: The Polyakov loop (a) and Polyakov loop susceptibility (b) as a function of temperature for different values of imaginary angular velocity Ω_I. The results are obtained on the lattice $8 \times 24 \times 49^2$.

- The height of the peak $\chi^{(max)}$ slightly grows with angular velocity for OBC.

Periodic boundary conditions

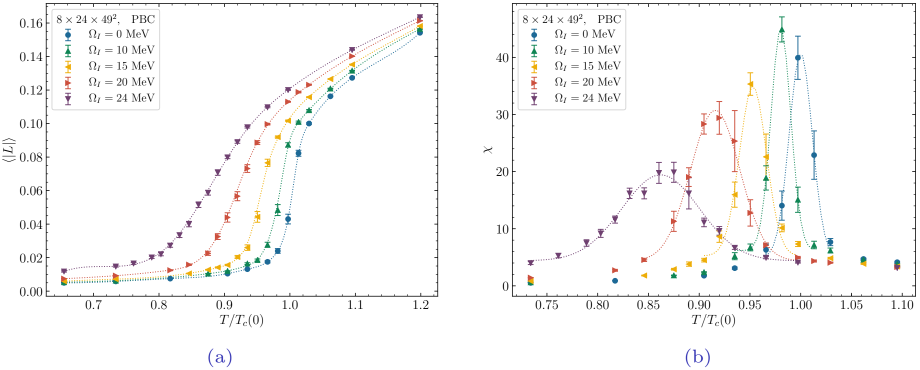

Figure: The Polyakov loop (a) and Polyakov loop susceptibility (b) as a function of temperature for different values of imaginary angular velocity Ω_I. The results are obtained on the lattice $8 \times 24 \times 49^2$.

- The height of the peak $\chi^{(max)}$ falls down with angular velocity.

Dirichlet boundary conditions

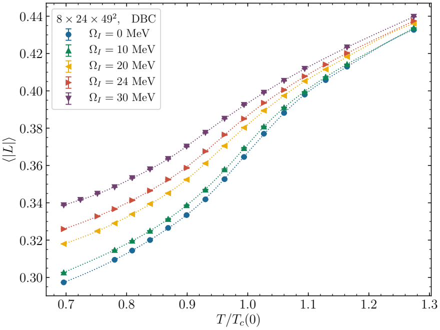

(a)

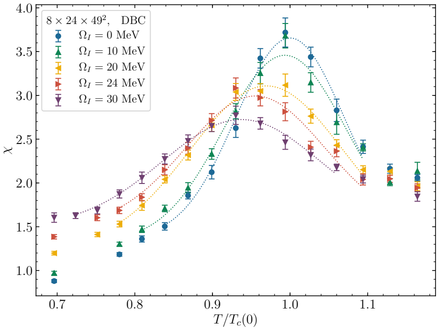

(b)

Figure: The Polyakov loop (a) and Polyakov loop susceptibility (b) as a function of temperature for different values of imaginary angular velocity Ω_I. The results are obtained on the lattice $8 \times 24 \times 49^2$.

- The height of the Polyakov loop susceptibility $\chi^{(max)}$ falls down with rotation.
- Polyakov loop is not zero for low temperatures. Contribution from boundary is $\delta L_{b.c.} = 12(N_s - 1)/N_s^2$, or $\delta L_{b.c.} \simeq 0.24$.

Open boundary conditions: Polyakov loop distribution

The local Polyakov loop in x, y-plane

$$L(x,y) = \frac{1}{N_z} \sum_z L(x,y,z)$$

Open boundary conditions: Polyakov loop distribution

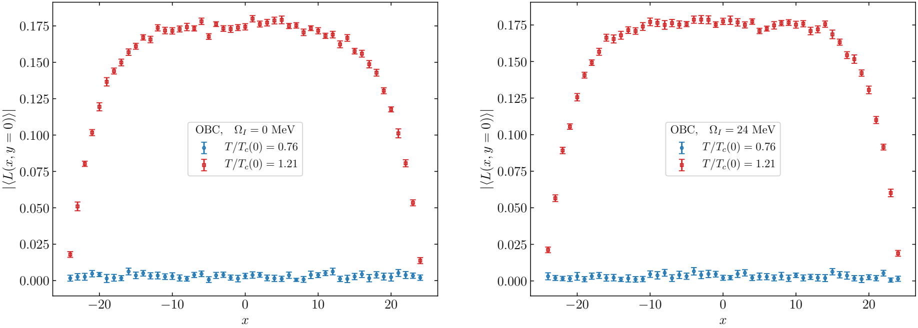

Figure: The local Polyakov loop $|\langle L(x,y)\rangle|$ as a function of coordinate for OBC and $\Omega_I = 0$ MeV (left), $\Omega_I = 24$ MeV (right). Points with $x \neq 0, y = 0$ from the lattice $8 \times 24 \times 49^2$ are shown.

- The local Polyakov loop $|\langle L(x,y)\rangle|$ is zero for all spatial points in the confinement phase, both with and without rotation $\Rightarrow$ Polyakov loop still acts as the order parameter.
- In deconfinement phase the boundary is screened.

Periodic boundary conditions: Polyakov loop distribution

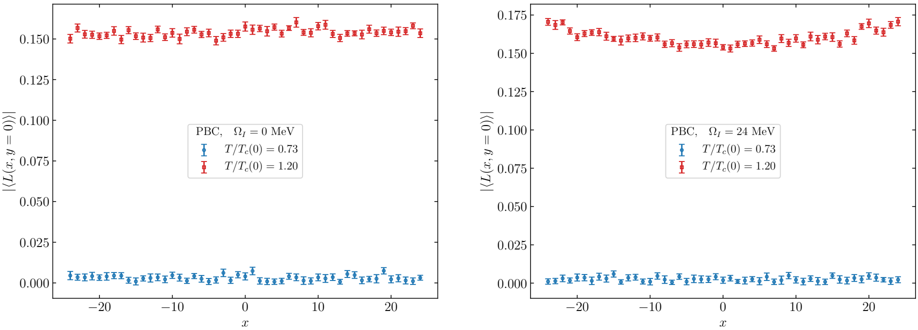

Figure: The local Polyakov loop $|\langle L(x,y)\rangle|$ as a function of coordinate for OBC and $\Omega_I = 0$ MeV (left), $\Omega_I = 24$ MeV (right). Points with $x \neq 0, y = 0$ from the lattice $8 \times 24 \times 49^2$ are shown.

- The local Polyakov loop $|\langle L(x,y)\rangle|$ is zero for all spatial points in the confinement phase, both without rotation and with nonzero angular velocity.
- The local Polyakov loop demonstrates weak dependence on the coordinate in the deconfinement phase.

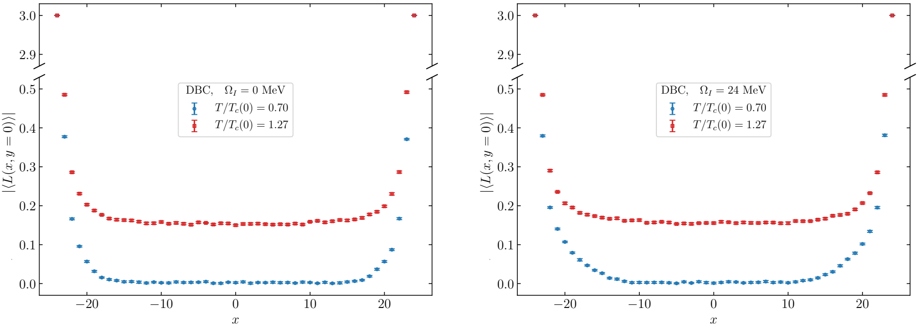

Figure: The local Polyakov loop $|\langle L(x, y)\rangle|$ as a function of coordinate for OBC and $\Omega_I = 0$ MeV (left), $\Omega_I = 24$ MeV (right). Points with $x \neq 0, y = 0$ from the lattice $8 \times 24 \times 49^2$ are shown.

- The local Polyakov loop $|\langle L(x, y)\rangle|$ is equal three on the boundary in both phases.
- The boundary is screened.